

Accepted Article

Title: Construction of Self-Reporting Biodegradable CO₂-based Polycarbonates for the Visualization of Thermoresponsive Behavior with Aggregation-Induced Emission Technology

Authors: Molin Wang, Enhao Wang, Han Cao, Shunjie Liu,* Xianhong Wang,* and Fosong Wang

This manuscript has been accepted and appears as an Accepted Article online.

This work may now be cited as: *Chin. J. Chem.* **2021**, *39*, 10.1002/cjoc.202100372.

The final Version of Record (VoR) of it [with formal page numbers](#) will soon be published online in Early View: <http://dx.doi.org/10.1002/cjoc.202100372>.

Construction of Self-Reporting Biodegradable CO₂-based Polycarbonates for the Visualization of Thermoresponsive Behavior with Aggregation-Induced Emission Technology

Molin Wang,^{a,b} Enhao Wang,^{a,b} Han Cao,^{a,b} Shunjie Liu,^{*a,b} Xianhong Wang,^{*a,b} and Fosong Wang^{a,b}

^aKey Laboratory of Polymer Ecomaterials, Changchun Institute of Applied Chemistry, Chinese Academy of Sciences, Changchun, 130022, China.

^bSchool of Applied Chemistry and Engineering, University of Science and Technology of China, Hefei, 230026, China

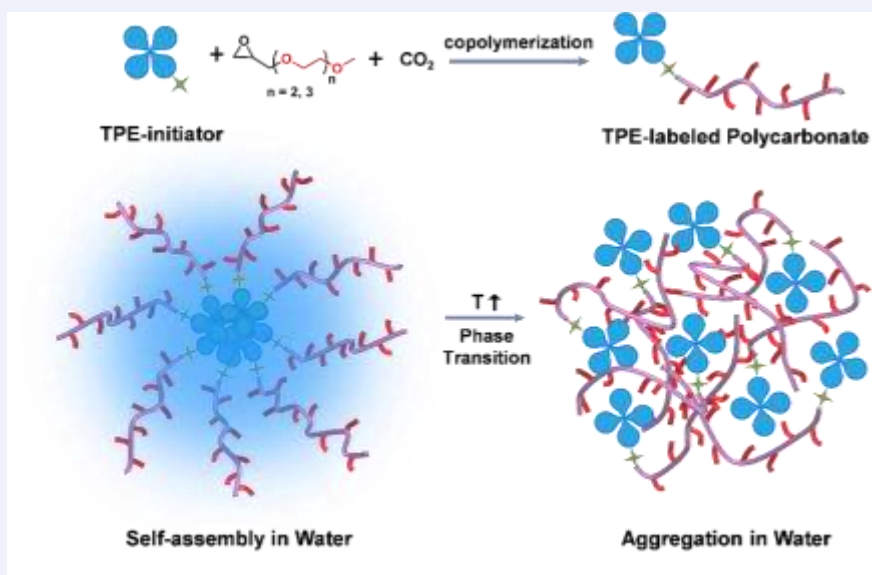
Keywords

CO₂ copolymerization | polycarbonates | thermoresponsive polymers | aggregation-induced emission | visualization

Main observation and conclusion

Thermoresponsive polymers with simultaneous biodegradability and signal “self-reporting” outputs that meet for advanced applications are hard to obtain. To address this issue, we developed fluorescence signal “self-reporting” biodegradable thermoresponsive polycarbonates through the immortal copolymerization of CO₂ and oligoethylene glycol monomethyl ether-functionalized epoxides in the presence of hydroxyl-modified tetraphenylethylene (TPE-OH). TPE-OH was used as chain transfer agent to afford well-defined polycarbonates with controlled molecular weight (6000 ~ 17000 g mol⁻¹) and aggregation-induced emission characteristics. Through temperature-dependent fluorescence intensity study, low critical solution transition of TPE-labeled polycarbonates were determined and the fine details of thermal-induced phase transition process were monitored. Further research indicated that temperature-controlled aggregation and dissociation of TPE moieties are the main reason for fluorescence intensity variations. We anticipate that this work could offer a method to visualize the thermal transition process of thermoresponsive polycarbonates and broaden their application fields as smart materials.

Comprehensive Graphic Content



*E-mail: sjliu@ciac.ac.cn, xhwang@ciac.ac.cn

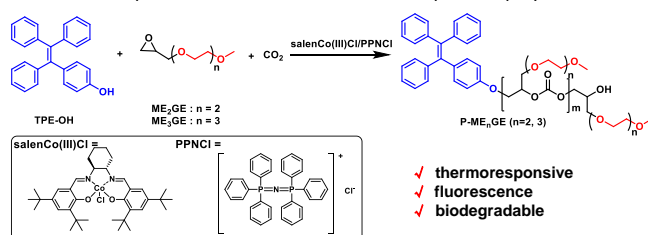
Background and Originality Content

Stimuli-responsive polymers are capable of responding “smartly” with rapid physical or chemical transition to the external stimuli, such as temperature, light, pH, electric field and ionic strength.^[1-2] Among them, thermoresponsive polymers with lower critical solution temperature (LCST) close to the body temperature have shown a wide range of biomedical applications as drug delivery, tissue engineering, and gene therapy due to their unique properties.^[3] For this purpose, many thermoresponsive polymers have been developed such as poly(N-isopropylacrylamide) (PNIPAM),^[4-7] poly(N-vinyl caprolactam) (PNVCL),^[8-9] poloxamers^[10] and polyoxazolines,^[11-13] etc. However, the non-biodegradability issue hinders the *in vivo* applications. Despite strategies such as copolymerization with biodegradable monomers^[14-15] or post-polymerization modification^[16-17] partially improve the biodegradability, the main architecture of the resulting materials still suffers from incomplete degradation.^[18] Therefore, it is of great significance to develop thermoresponsive polymers with complete biodegradability.

Copolymerization of carbon dioxide (CO₂) and epoxides into polycarbonates is regarded as a valid way to synthesize biodegradable polymers.^[19-22] On the basis of the breakthrough in catalyst design, various polycarbonates derived from different types of epoxides have been successfully developed.^[23-30] Through copolymerization of a hydrophilic oligoethylene glycol monomethyl ether (OEG) functionalized epoxide (a thermoresponsive unit) with CO₂, Wang and coworkers successfully synthesized biodegradable thermoresponsive polycarbonates.^[31] However, the topological architecture and molecular weight of the resulting polymers are hard to control, owing to the incorporation of the third epoxide monomer.^[32] Moreover, just like common thermoresponsive polymers, the as-prepared biodegradable polycarbonates lack accessible methods to rapidly and facily reflect the microscopic changes into visible or detectable signals, which make them difficult to become high value-added materials.^[33] Therefore, it remains challenging to prepare biodegradable thermoresponsive polycarbonates with well-defined architecture and self-reporting signal outputs.

In this work, herein, to address the above issues, we developed fluorescence

Scheme 1. Preparation of TPE-labeled thermoresponsive polycarbonates



signal “self-reporting” biodegradable thermoresponsive polycarbonates through the copolymerization of CO₂ and OEG-functionalized epoxides in the presence of hydroxyl-modified tetraphenylethylene (TPE-OH) (Scheme 1). The binary (salen)Co(III)Cl/PPNCl complex was utilized to afford polycarbonates with completely alternating structure which assures biodegradability.^[34-35] The role of TPE-OH is of key importance. On the one hand, it possesses unique aggregation-induced emission (AIE) attributes,^[36-37] which can change the fluorescence intensity through the restriction of intramolecular motion (RIM) mechanism subjected to thermal stimulus.^[38] On the other hand, TPE-OH acts as chain transfer agent (CTA) to give polycarbonates good adjustability of molecular weight via the mechanism of immortal polymerization.^[39] Therefore, the molecular weight of TPE-labeled thermoresponsive polymer can be well controlled in the range of 6000 ~ 17000 g mol⁻¹. The thermoresponsive process of TPE-labeled polycarbonates is reflected by fluorescence signal in real time. Most importantly, through the derivative analysis of the fluorescence curves, the fine temperature variation which responds to the microstructure’s transformation of the polymer can be facily visualized. Collectively, the present study provides a new strategy to design fluorescence self-reporting thermoresponsive polymers.

Results and Discussion

Synthesis and Characterization of TPE-Labeled Thermoresponsive Polycarbonates.

Table 1. The copolymerization of epoxide/CO₂ catalyzed by SalenCoCl/PPNCl using TPE-OH as CTA

Entry ^a	monomer	feed ^b	polymer (%) ^c	CU (%) ^d	M _n (g mol ⁻¹) ^e	Đ
1	ME ₂ GE	400/1/1/1	94	99	17100	1.21
2	ME ₂ GE	400/1/1/2	93	99	11300	1.24
3	ME ₂ GE	400/1/1/5	93	99	8100	1.23
4	ME ₂ GE	400/1/1/10	93	99	6400	1.17
5	ME ₃ GE	400/1/1/1	93	99	17900	1.20
6	ME ₃ GE	400/1/1/2	93	99	15400	1.18
7	ME ₃ GE	400/1/1/5	89	99	9700	1.18
8	ME ₃ GE	400/1/1/10	89	99	7500	1.15

^a The polymerization reactions were carried out in 2.0 mL of epoxides in 10 mL autoclaves, at 25°C and 3.0 MPa CO₂. Note: to make sure the complete conversion of epoxide monomer (> 99%), the reaction time of all polymerizations was set as 12h. ^b The molar ratio of monomer: salenCoCl: PPNCl: TPE-OH. ^c Selectivity of polycarbonate over cyclic carbonate. ^d Determined by ¹H NMR spectroscopy. ^e Determined by gel-permeation chromatography in

CH₂Cl₂ at 35 °C calibrated with polystyrene standards.

TPE-labeled thermoresponsive polycarbonates are synthesized by immortal copolymerization of CO₂/OEG-functionalized epoxides using SalenCo(III)Cl/PPNCl catalyst system in the presence of TPE-OH CTA. As illustrated in **Scheme 1**, to improve the hydrophilicity, two kinds of epoxides, ME₂GE and ME₃GE, bearing different length of OEG were utilized to prepare thermoresponsive polycarbonates P-ME_nGE (*n* = 2, 3), where *n* represents the number of repeating units in the pendent OEG chains. The results of immortal copolymerizations of CO₂/ME_nGE (*n* = 2, 3) are summarized in **Table 1**. All the reactions were carried out with [epoxides]/[Co center] molar ratio of 400:1 at 25 °C under CO₂ pressure of 3.0 MPa. To ensure the complete monomer conversion (> 99%), the reaction time was optimized to 12 h. A series of P-ME_nGE (*n*=2, 3) with different number-average molecular weight (*M_n*) and relatively narrow molar mass dispersity (*Đ*) were prepared by adjusting monomer-to-initiator (TPE-OH + salenCoCl + PPNCl) ratios (M/I). As shown in entries 1~4 in **Table 1**, with the variation of M/I from 400: 1 to 400: 10, *M_n* of P-ME₂GE reduced gradually from 17100 g mol⁻¹ to 6400 g mol⁻¹ with a narrow *Đ* of ~1.2 (**Figure S1**). Similarly, in entries 5~8, the *M_n* of P-ME₃GE was controllable in the range of 17900 g mol⁻¹ to 7500 g mol⁻¹. It's worth noting that the carbonate units (CU) content remained at 99% in all reactions suggesting the nearly complete alternating structure. Moreover, the *M_n* of P-ME₂GE and P-ME₃GE displayed good linear relationships with of M/I (**Figure 1**), demonstrating the effective controllability of TPE-OH on the *M_n* of the resulting polymers.^[40] Altogether, well-defined TPE-labeled polycarbonates with OEG side chains were successfully obtained.

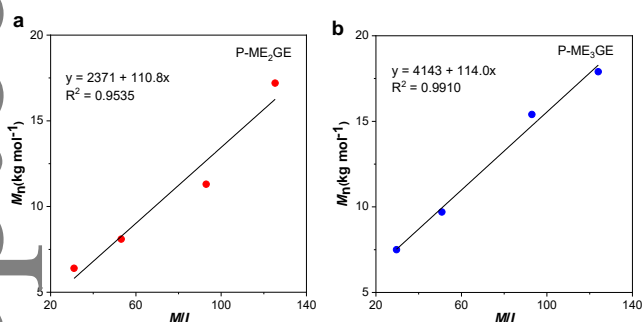


Figure 1. The relationship of *M_n* of the as-prepared polymer with M/I. (a) P-ME₂GE, (b) P-ME₃GE.

Chemical structures of intermediates and polymers were confirmed by ¹H NMR spectra (**Figure 2** and **Figure S2~S12**) and matrix-assisted laser desorption/ionization time-of-flight mass spectroscopy (MALDI-TOF). The characteristic peaks at 3.39, 3.56, and 3.60–3.75 ppm which corresponded to CH₃ and CH₂, respectively in ME₂GE and ME₃GE (**Figure 2a, b**), were clearly observed in polycarbonate P-ME_nGE (**Figure 2d, e**), indicating that the OEG chains were incorporated into the polymer backbone. In addition, characteristic peaks of TPE-OH (6.55–7.22 ppm in **Figure 2c**) were appeared in P-ME_nGE. Moreover, the strong signals at 5.04 and 4.15–4.55 ppm were ascribed to CH and CH₂ in carbonate units. Meanwhile, the absence of characteristic peaks of ether linkage (homopolymer of epoxides, at 3.30–3.60 ppm) suggested that the backbone of P-ME_nGE was completely alternating (CU content > 99%).^[41] MALDI-TOF spectroscopy showed the signals of two species, [TPE-O(P-ME₂GE)]Na⁺ (*n* = 9~24) and [TPE-O(P-ME₃GE)]Na⁺ (*n* = 8~26), again demonstrating the incorporation of TPE-OH into the polymer (**Figure S13, S14**). Altogether, the above results demonstrated the successful incorporation of TPE unit into the backbone of polycarbonates.

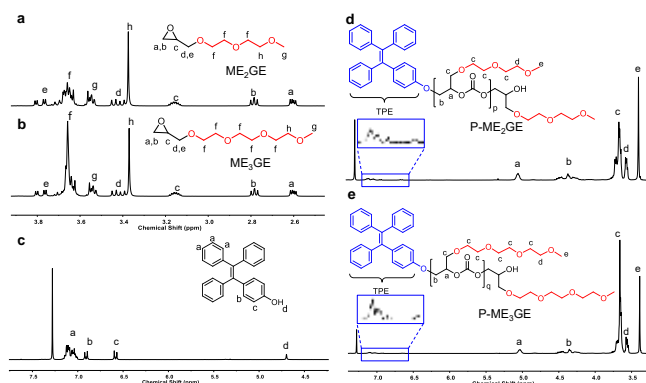


Figure 2. ¹H NMR spectra of samples (300 MHz, CDCl₃). (a) ME₂GE, (b) ME₃GE, (c) TPE-OH, (d) P-ME₂GE (*M_n* = 6400 g mol⁻¹), (e) P-ME₃GE (*M_n* = 7300 g mol⁻¹).

Thermoresponsive properties of fluorescent P-ME_nGE in Aqueous Solution.

The relationship between fluorescence properties and temperature response of P-ME_nGE (*n* = 2, 3) in aqueous solution was studied using temperature-dependent fluorescence spectrometer. Due to the hydrophilicity of OEG side chains, both of P-ME₂GE and P-ME₃GE could disperse into tiny micelles in aqueous solution at room temperature. The relationship between fluorescence properties and temperature response of P-ME_nGE (*n* = 2, 3) in aqueous solution was studied using temperature-dependent fluorescence spectrometer. Due to the hydrophilicity of OEG side chains, both of P-ME₂GE and P-ME₃GE exhibited good water solubility at room temperature. P-ME₂GE (*M_n* = 6400 g mol⁻¹) and P-ME₃GE (*M_n* = 7300 g mol⁻¹) with comparable molecular weight were chosen as examples to investigate their fluorescence-temperature properties. The aqueous solution of P-ME_nGE (0.5 mg mL⁻¹) exhibited obvious fluorescence emission, owing to the presence of TPE unit. Normally, P-ME_nGE tended to form micelles in aqueous solution where hydrophilic OEG chains stretched on the outside while hydrophobic TPE and carbonate units aggregated into cores. The hydrophobic aggregates trigger the RIM mechanism of TPE to give strong fluorescence.^[42-43] As shown in **Figure 3**, the two polymers showed fluorescence emission peak at ~464 nm in aqueous solution at room temperature under excitation of 321 nm (**Figure S15**). For P-ME₂GE (**Figure 4a**), fluorescence intensity generally showed a downward trend with the increase of temperature from 25 to 70 °C. The fluorescence intensity remained almost invariable at low temperature (25 to 32 °C), but showed an abrupt decrease in

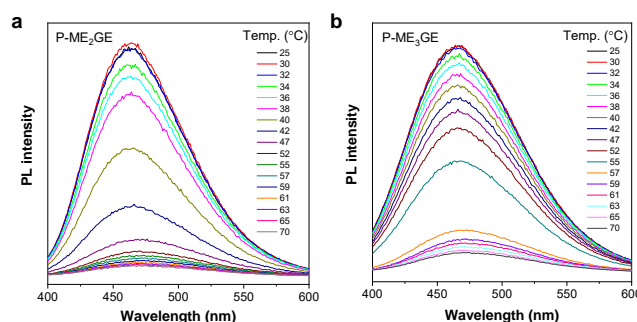


Figure 3. Temperature-dependent fluorescence spectra of aqueous solution of (a) P-ME₂GE (*M_n* = 6400 g mol⁻¹) and (b) P-ME₃GE (*M_n* = 7300 g mol⁻¹). Concentration: 0.5 mg mL⁻¹. λ_{ex} = 321 nm.

the range of 32 to 45 °C. Further increase to 60 °C led to the fluorescence quenching of P-ME₂GE. Therefore, upon phase transition, the self-reporting output is triggered and made visible by variations in fluorescence. Similar phenomena were also observed in P-ME₃GE aqueous solution and the rapid transition temperature range was 40–56 °C (Figure 4b). Presumably, these phenomena were caused by two reasons. On the one hand, the active intramolecular motion of TPE triggered by temperature resulted in enhanced nonradiative decay of the excited state and then weakened the fluorescence.^[44] On the other hand, the newly formed hydrophobic domains derived from dehydration of OEG side chains with temperature provided platform for the intramolecular motion of TPE.^[45]

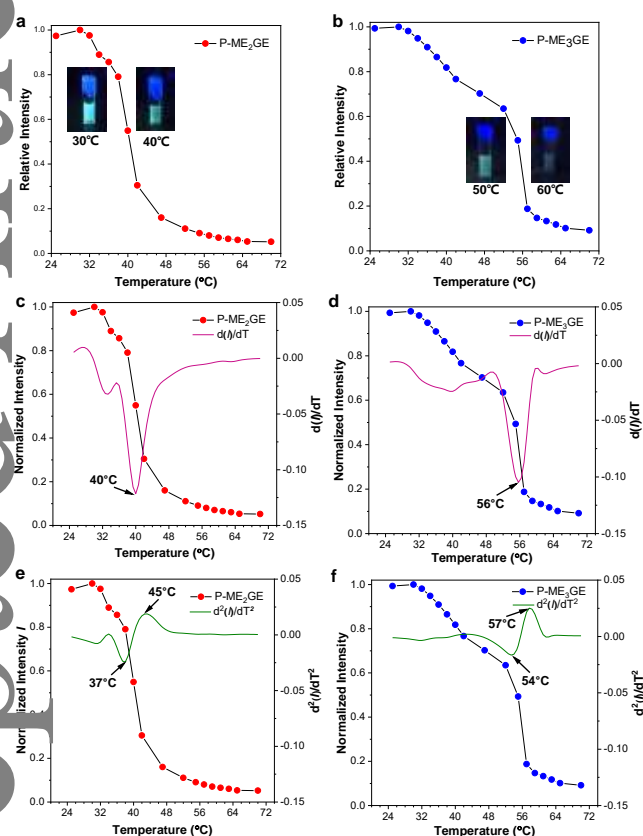


Figure 4. The relationship between fluorescence intensity at 464 nm with temperature. (a) P-ME₂GE and (b) P-ME₃GE. Inset: fluorescence photos at corresponding temperature. The first-order (c and d) and second-order (e and f) derivatives of temperature-dependent FL intensity curves for P-ME₂GE ($M_n = 6400 \text{ g mol}^{-1}$) and P-ME₃GE ($M_n = 7300 \text{ g mol}^{-1}$), respectively. Fluorescence intensity at 464 nm. Concentration: 0.5 mg mL^{-1} . $\lambda_{\text{ex}} = 321 \text{ nm}$.

To explore more details about the thermal-induced phase transition of P-ME_nGE, we performed the first-order and second-order derivatives of the temperature-dependent FL intensity curves (Figure 4c, d, e, f). The minimum value of the first-order derivative represented the temperature at which the FL intensity changed most significantly, which is 40 °C and 55 °C for P-ME₂GE and P-ME₃GE, respectively. Meanwhile, there were minimum and maximum in the second derivatives owing to the rapid decrease in fluorescence intensity,^[46] which was related to the thermal-induced phase transition of the polymers. The aqueous solution of thermoresponsive polymers with LCST could show cloud point on heating procedure. We defined 37 °C and 54 °C as the cloud point for P-ME₂GE and P-ME₃GE respectively. At the minimum temperature, the OEG side chains of P-ME_nGE

began to dehydrate and induce phase transition. While, at the maximum temperature the polymer chains were almost completely dehydrated indicating the finish of the phase transition.^[47] Thanks to the AIE characteristics of TPE moieties, temperature changes were monitored sensitively and the fine details were revealed during the thermal-induced phase transition of thermoresponsive polymer aqueous solution.

The Phase Transition Behaviors of TPE-Labeled Polycarbonates in water under various Temperatures.

The morphologies of P-ME_nGE ($n = 2, 3$) in aqueous solution at different temperature were characterized by dynamic light scattering (DLS). As exhibited in Figure 5a, the aqueous solution of P-ME₂GE self-assembled into micelles with hydrodynamic diameters (D_h) of about 20 nm at room temperature. The D_h of micelles kept constant (20 nm) with an increase of temperature to 35 °C. However, when temperature reached above 40 °C, D_h of micelles leaped to 500 nm because of the aggregation of dehydrated polymer chains.^[48] This significant fluctuation of D_h with temperature in the range of 35–40 °C properly exhibited the thermal transition process of P-ME₂GE near cloud point. In Figure 5b, the D_h of P-ME₃GE micelles remained stable at 50–55 °C while showed a significant increase at 60 °C, indicating the cloud point (54 °C) of P-ME₃GE from molecular aggregation level. These re-

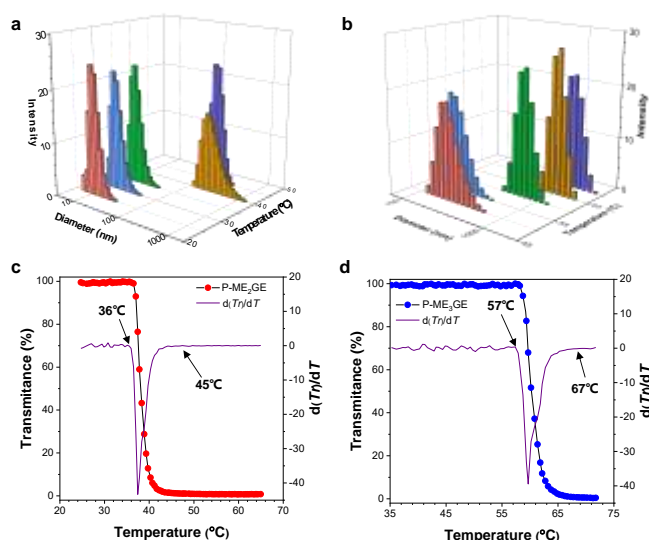


Figure 5. Hydrodynamic diameters of P-ME₂GE (a) and P-ME₃GE (b) in aqueous solution at different temperatures determined by DLS. Concentration: 0.5 mg mL^{-1} . Temperature-dependent transmittance of aqueous solutions of P-ME₂GE (c) and P-ME₃GE (d) at 500 nm with the first-order derivative of the corresponding curves.

sults were consistent with the above temperature-dependent FL intensity study.

Common temperature-dependent optical transmittance tests were also conducted to further confirm the thermal transition properties of P-ME_nGE ($n = 2, 3$) (Figure 5c, d). According to UV-vis spectra of P-ME_nGE in aqueous solution (Figure S15), we chose 500 nm to measure the transmittance of polymer solution in order to avoid the interference of TPE absorption. The transmittance of solution dropped rapidly until it reached zero. The first-order derivative of transmittance curves displayed a sharp inverted peak, indicating a thermal transition temperature of the polymers. The temperature variation range of 36 to 45 °C in P-ME₂GE was in good agreement with the fluorescence results (37–45 °C). However, the result of P-ME₃GE deviated from the fluorescence data, which might be attributed to the fact that the

influence of molecular motion on TPE fluorescence intensity was more obvious at high temperature.^[49]

To further investigate the micro-changes of P-ME_nGE during thermal-induced phase transition, ¹H-NMR measurement were conducted in D₂O at various temperatures. **Figure 6** shows the ¹H-NMR spectra of P-ME₂GE in D₂O during the heating process from 25 to 50 °C. All spectra were measured under the same parameters and the signal of water at 4.79 ppm was taken as internal reference. At low temperature (25~30 °C), the signals assigned to OEG units

(3.20-3.80 ppm) were strong and clear, indicating the flexible movements of the protons in OEG side chains.^[50] At high temperature (36-50 °C), the proton peaks became broader. It means that the mobility of protons were restricted because of polymer's collapse by the dehydration of OEG side chains.^[51] This result was in consistent with the thermal transition behavior measured by fluorescence and transmittance methods. However, an opposite variation trend was observed in TPE moiety. At low temperature (25~30 °C), the proton peaks of TPE remained broad, while the peaks split into multiple peaks at high temperatures (36-50 °C), which was resulted from the enhanced intramolecular motion of TPE with temperature. The downfield-shifted proton peaks both in OEG and TPE moieties were possible due to the gradual breakdown of polymer-water hydrogen bonds.^[52] The ¹H-NMR spectra of P-ME₃GE also display similar variation pattern (**Figure S16**). These results confirmed the special role of TPE in fluorescence self-reporting the thermal transition process of polymers.

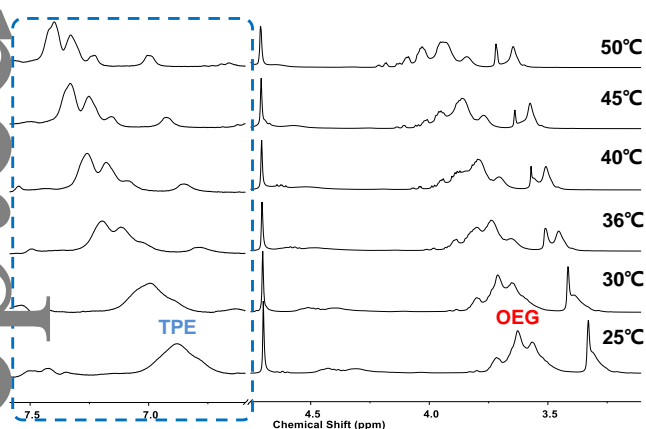


Figure 6. ¹H NMR spectra of P-ME₂GE in D₂O at various temperatures. The proton peaks of TPE moiety in the dotted box is enlarged for clarity.

To investigate the degradability of P-ME_nGE, the *in vitro* hydrolytic degradation of P-ME₂GE ($M_n=6400 \text{ g mol}^{-1}$) was carried out in an aqueous solution at room temperature with a concentration of 0.5 mg mL⁻¹. The process of degradation was observed by ¹H NMR spectra in D₂O. As shown in **Figure S17**, the characteristic peaks at 4.95, 4.54 and 4.30 ppm belonging to cyclic carbonates were observed after 15 days, which indicated that the polymer has been partially degraded. The polymers with similar structures to PC-ME_nGE also showed good degradability in neutral pH condition.^[31] This result suggested the potential applications of P-ME_nGE in biodegradable materials.

Conclusions

In conclusion, we have successfully synthesized thermoresponsive CO₂-based biodegradable polycarbonates P-ME_nGE ($n=2, 3$) with well-defined architectures and AIE characteristics by copolymerization of CO₂ and OEG-functionalized epoxides using TPE-OH as chain transfer agent. The role of TPE-OH was of key

importance. First, it enables polymer with controlled molecular weight from 6400 to 17100 g mol⁻¹ for P-ME₂GE and 7500 to 17900 for P-ME₃GE by regulating the feeding ratio of M/I. Second, the AIE attributes of TPE-OH realized the fluorescence self-reporting of the thermoresponsive transition of polymers according to the intramolecular mobility-dependent fluorescence. The self-assembly of TPE-labeled polymer in aqueous solution resulted in fluorescence enhancement owing to the RIM mechanism of TPE. Through temperature-dependent fluorescence intensity study, the cloud points of P-ME₂GE and P-ME₃GE were determined to be 37 and 54 °C, respectively. The derivative analysis of the fluorescence intensity curve revealed the whole thermal transition process with temperature owing to the dehydration of OEG units. The present study may provide a self-reporting method to visualize the thermal transition process of biodegradable thermoresponsive polymers.

Experimental

All the experimental details are provided in supporting information.

Supporting Information

The supporting information for this article is available on the WWW under <https://doi.org/10.1002/cjoc.2021xxxx>.

Acknowledgement

The authors acknowledge the financial support from Fundamental Science Center projector in National Natural Science Foundation of China (Grant No. 51988102), and Key Research Program of Frontier Sciences, CAS (Grant No. QYZDJ-SSW-JSC017). The authors also thanks Prof. Anjun Qin and Dr. Han Zhang in South China University of Technology for performing temperature-dependent fluorescence spectrometer.

References

- [1] Roy, D.; Brooks, W. L.; Sumerlin, B. S. New directions in thermoresponsive polymers. *Chem. Soc. Rev.* **2013**, *42*, 7214-7243.
- [2] Weng, C.; Fan, N.; Xu, T.; Chen, H.; Li, Z.; Li, Y.; Tan, H.; Fu, Q.; Ding, M. FRET-based polymer materials for detection of cellular microenvironments. *Chin. Chem. Lett.* **2020**, *31*, 1490-1498.
- [3] Wei, M.; Gao, Y.; Li, X.; Serpe, M. J. Stimuli-responsive polymers and their applications. *Polym. Chem.* **2017**, *8*, 127-143.
- [4] Wu, C.; Wang, X. Globule-to-coil transition of a single homopolymer chain in solution. *Phys. Rev. Lett.* **1998**, *80*, 4092-4094.
- [5] Zhang, Y.; Furryk, S.; Bergbreiter, D. E.; Cremer, P. S. Specific ion effects on the water solubility of macromolecules: PNIPAM and the Hofmeister series. *J. Am. Chem. Soc.* **2005**, *127*, 14505-14510.
- [6] Xian, C.; Yuan, Q.; Bao, Z.; Liu, G.; Wu, J. Progress on intelligent hydrogels based on RAFT polymerization: Design strategy, fabrication and the applications for controlled drug delivery. *Chin. Chem. Lett.* **2020**, *31*, 19-27.
- [7] Heskins, M.; Guillet, J. E. Solution Properties of Poly(N-isopropylacrylamide). *J. Macromol. Sci. Chem.* **1968**, *2*, 1441-1455.
- [8] Tager, A. A.; Safronov, A. P.; Berezyuk, E. A.; Galaev, I. Y. Lower Critical Solution Temperature and Hydrophobic Hydration in Aqueous Polymer-Solutions. *Colloid. Polym. Sci.* **1994**, *272* (10), 1234-1239.
- [9] Ramos, J.; Imaz, A.; Forcada, J. Temperature-sensitive nanogels: poly(N-vinylcaprolactam) versus poly(N-isopropylacrylamide). *Polym. Chem.* **2012**, *3*, 852-856.
- [10] Hwang, M. J.; Suh, J. M.; Bae, Y. H.; Kim, S. W.; Jeong, B. Caprolactonic poloxamer analog: PEG-PCL-PEG. *Biomacromolecules* **2005**, *6*, 885-890.

- [11] Park, J.-S.; Kataoka, K. Comprehensive and Accurate Control of Thermo-sensitivity of Poly(2-alkyl-2-oxazolines) via Well-Defined Gradient or Random Copolymerization. *Macromolecules* **2007**, *40*, 3599-3609.
- [12] Park, J. S.; Akiyama, Y.; Winnik, F. M.; Kataoka, K. Versatile synthesis of end-functionalized thermosensitive poly(2-isopropyl-2-oxazolines). *Macromolecules* **2004**, *37*, 6786-6792.
- [13] Liu, L.; Yin, L.; Bian, H.; Zhang, N. Polymeric nanoparticles of poly(2-oxazoline), tannic acid and doxorubicin for controlled release and cancer treatment. *Chin. Chem. Lett.* **2020**, *31*, 501-504
- [14] Yang, J.; van Lith, R.; Baler, K.; Hoshi, R. A.; Ameer, G. A. A thermoresponsive biodegradable polymer with intrinsic antioxidant properties. *Biomacromolecules* **2014**, *15*, 3942-3952.
- [15] Swanson, J. P.; Martinez, M. R.; Cruz, M. A.; Mankoci, S. G.; Costanzo, P. J.; Joy, A. A cocervate-forming biodegradable polyester with elevated LCST based on bis-(2-methoxyethyl) amine. *Polym. Chem.* **2016**, *7*, 4693-4702.
- [16] Gupta, M. K.; Martin, J. R.; Werfel, T. A.; Shen, T.; Page, J. M.; Duvall, C. L. Cell protective, ABC triblock polymer-based thermoresponsive hydrogels with ROS-triggered degradation and drug release. *J. Am. Chem. Soc.* **2014**, *136*, 14896-14902.
- [17] Thomas, A. W.; Kuroishi, P. K.; Perez-Madrigal, M. M.; Whittaker, A. K.; Dove, A. P. Synthesis of aliphatic polycarbonates with a tuneable thermal response. *Polym. Chem.* **2017**, *8*, 5082-5090.
- [18] Li, Y.; Liu, S.; Zhao, X.; Wang, Y.; Liu, J.; Wang, X.; Lu, L. CO₂-based amphiphilic polycarbonate micelles enable a reliable and efficient platform for tumor imaging. *Theranostics* **2017**, *7*, 4689-4698.
- [19] Zhu, Y.; Romain, C.; Williams, C. K. Sustainable polymers from renewable resources. *Nature* **2016**, *540*, 354-362.
- [20] Kozak, C. M.; Ambrose, K.; Anderson, T. S. Copolymerization of carbon dioxide and epoxides by metal coordination complexes. *Coord. Chem. Rev.* **2018**, *376*, 565-587.
- [21] Klaus, S.; Lehenmeier, M. W.; Anderson, C. E.; Rieger, B. Recent advances in CO₂/epoxide copolymerization-New strategies and cooperative mechanisms. *Coord. Chem. Rev.* **2011**, *255*, 1460-1479.
- [22] Grignard, B.; Gennen, S.; Jerome, C.; Kleij, A. W.; Detrembleur, C. Advances in the use of CO₂ as a renewable feedstock for the synthesis of polymers. *Chem. Soc. Rev.* **2019**, *48*, 4466-4514.
- [23] Zhang, D.; Boopathi, S. K.; Hadjichristidis, N.; Gnanou, Y.; Feng, X. Metal-Free Alternating Copolymerization of CO₂ with Epoxides: Fulfilling "Green" Synthesis and Activity. *J. Am. Chem. Soc.* **2016**, *138*, 11117-11120.
- [24] Chen, Z.; Yang, J.; Lu, X.; Hu, L.; Cao, X.; Wu, G.; Zhang, X. Triethyl borane-regulated selective production of polycarbonates and cyclic carbonates for the coupling reaction of CO₂ with epoxides. *Polym. Chem.* **2019**, *10*, 3621-3628.
- [25] Yang, G.; Zhang, Y.; Xie, R.; Wu, G. Scalable Bifunctional Organoboron Catalysts for Copolymerization of CO₂ and Epoxides with Unprecedented Efficiency. *J. Am. Chem. Soc.* **2020**, *142*, 12245-12255.
- [26] Garden, J. A.; Saini, P. K.; Williams, C. K. Greater than the Sum of Its Parts: A Heterodinuclear Polymerization Catalyst. *J. Am. Chem. Soc.* **2015**, *137*, 15078-15081.
- [27] Liu, Y.; Zhou, H.; Guo, J.; Ren, W.; Lu, X. Completely Recyclable Monomers and Polycarbonate: Approach to Sustainable Polymers. *Angew. Chem. Int. Ed. Engl.* **2017**, *56*, 4862-4866.
- [28] Darensbourg, D. J.; Wei, S.; Yeung, A. D.; Ellis, W. C. An Efficient Method of Depolymerization of Poly(cyclopentene carbonate) to Its Comonomers: Cyclopentene Oxide and Carbon Dioxide. *Macromolecules* **2013**, *46*, 5850-5855.
- [29] Kissling, S.; Lehenmeier, M. W.; Altenbuchner, P. T.; Kronast, A.; Reiter, M.; Deglmann, P.; Seemann, U. B.; Rieger, B. Dinuclear zinc catalysts with unprecedented activities for the copolymerization of cyclohexene oxide and CO₂. *Chem. Commun. (Camb)* **2015**, *51*, 4579-4582.
- [30] Wu, G.; Wei, S.; Ren, W.; Lu, X.; Xu, T.; Darensbourg, D. J. Perfectly alternating copolymerization of CO₂ and epichlorohydrin using cobalt(III)-based catalyst systems. *J. Am. Chem. Soc.* **2011**, *133*, 15191-15199.
- [31] Zhou, Q.; Gu, L.; Gao, Y.; Qin, Y.; Wang, X.; Wang, F. Biodegradable CO₂-based polycarbonates with rapid and reversible thermal response at body temperature. *J. Polym. Sci. Pol. Chem.* **2013**, *51*, 1893-1898.
- [32] Gu, L.; Qin, Y.; Gao, Y.; Wang, X.; Wang, F. Hydrophilic CO₂-based biodegradable polycarbonates: Synthesis and rapid thermo-responsive behavior. *J. Polym. Sci. Pol. Chem.* **2013**, *51*, 2834-2840.
- [33] Wang, Y.; Darensbourg, D. J. Carbon dioxide-based functional polycarbonates: Metal catalyzed copolymerization of CO₂ and epoxides. *Coord. Chem. Rev.* **2018**, *372*, 85-100.
- [34] Cao, H.; Wang, X. Carbon Dioxide Copolymer From Delicate Metal Catalyst: New Structure Leading to Practical Performance. In *Synthetic Polymer Chemistry: Innovations and Outlook*, RSC Publishing, **2020**, pp. 197-242
- [35] Paddock, R. L.; Nguyen, S. T. Alternating copolymerization of CO₂ and propylene oxide catalyzed by Co-III(salen)/Lewis base. *Macromolecules* **2005**, *38*, 6251-6253.
- [36] Dong, J.; Li, X.; Zhang, K.; Di Yuan, Y.; Wang, Y.; Zhai, L.; Liu, G.; Yuan, D.; Jiang, J.; Zhao, D. Confinement of Aggregation-Induced Emission Molecular Rotors in Ultrathin Two-Dimensional Porous Organic Nanosheets for Enhanced Molecular Recognition. *J. Am. Chem. Soc.* **2018**, *140*, 4035-4046.
- [37] Han, T.; Yan, D.; Wu, Q.; Song, N.; Zhang, H.; Wang, D. Aggregation-Induced Emission: A Rising Star in Chemistry and Materials Science. *Chin. J. Chem.* **2021**, *39*, 677-689.
- [38] Leung, N. L.; Xie, N.; Yuan, W.; Liu, Y.; Wu, Q.; Peng, Q.; Miao, Q.; Lam, J. W.; Tang, B. Z. Restriction of intramolecular motions: the general mechanism behind aggregation-induced emission. *Chemistry* **2014**, *20*, 15349-15353.
- [39] Wang, E.; Liu, S.; Lam, J. W. Y.; Tang, B. Z.; Wang, X.; Wang, F. Deciphering Structure-Functionality Relationship of Polycarbonate-Based Polyelectrolytes by AIE Technology. *Macromolecules* **2020**, *53*, 5839-5846.
- [40] Cyriac, A.; Lee, S. H.; Varghese, J. K.; Park, E. S.; Park, J. H.; Lee, B. Y. Immortal CO₂/Propylene Oxide Copolymerization: Precise Control of Molecular Weight and Architecture of Various Block Copolymers. *Macromolecules* **2010**, *43*, 7398-7401.
- [41] Ohkawara, T.; Suzuki, K.; Nakano, K.; Mori, S.; Nozaki, K. Facile estimation of catalytic activity and selectivities in copolymerization of propylene oxide with carbon dioxide mediated by metal complexes with planar tetradentate ligand. *J. Am. Chem. Soc.* **2014**, *136*, 10728-10735.
- [42] Peng, H.; Liu, B.; Wei, P.; Zhang, P.; Zhang, H.; Zhang, J.; Li, K.; Li, Y.; Cheng, Y.; Lam, J. W. Y.; Zhang, W.; Lee, C. S.; Tang, B. Z. Visualizing the Initial Step of Self-Assembly and the Phase Transition by Stereogenic Amphiphiles with Aggregation-Induced Emission. *ACS Nano* **2019**, *13*, 839-846.
- [43] Liu, S.; Cheng, Y.; Zhang, H.; Qiu, Z.; Kwok, R. T. K.; Lam, J. W. Y.; Tang, B. Z. In Situ Monitoring of RAFT Polymerization by Tetraphenylethylene-Containing Agents with Aggregation-Induced Emission Characteristics. *Angew. Chem. Int. Ed. Engl.* **2018**, *57*, 6274-6278.
- [44] Liu, S.; Ou, H.; Li, Y.; Zhang, H.; Liu, J.; Lu, X.; Kwok, R. T. K.; Lam, J. W. Y.; Ding, D.; Tang, B. Z. Planar and Twisted Molecular Structure Leads to the High Brightness of Semiconducting Polymer Nanoparticles for NIR-IIa Fluorescence Imaging. *J. Am. Chem. Soc.* **2020**, *142*, 15146-15156.
- [45] Lai, C. T.; Chien, R. H.; Kuo, S. W.; Hong, J. L. Tetraphenylthiophene-Functionalized Poly(N-isopropylacrylamide): Probing LCST with Aggregation-Induced Emission. *Macromolecules* **2011**, *44*, 6546-6556.
- [46] Qiu, Z.; Chu, E. K. K.; Jiang, M.; Gui, C.; Xie, N.; Qin, W.; Alam, P.; Kwok, R. T. K.; Lam, J. W. Y.; Tang, B. Z. A Simple and Sensitive Method for an Important Physical Parameter: Reliable Measurement of Glass Transition Temperature by AIEgens. *Macromolecules* **2017**, *50*, 7620-7627.
- [47] Tang, L.; Jin, J. K.; Qin, A.; Yuan, W. Z.; Mao, Y.; Mei, J.; Sun, J. Z.; Tang, B. Z. A fluorescent thermometer operating in aggregation-induced emission mechanism: probing thermal transitions of PNIPAM in water. *Chem. Commun. (Camb)* **2009**, 4974-4976.
- [48] Jiang, X.; Smith, M. R.; Baker, G. L. Water-soluble thermoresponsive poly lactides. *Macromolecules* **2008**, *41*, 318-324.
- [49] Jia, Y.; Chen, K.; Gao, M.; Liu, S.; Wang, J.; Chen, X.; Wang, L.; Chen, Y.; Song, W.; Zhang, H.; Ren, L.; Zhu, X.; Tang, B. Z. Visualizing phase transition of upper critical solution temperature (UCST) polymers

with AIE. *Sci. China. Chem.* **2021**, *64*, 403-407.

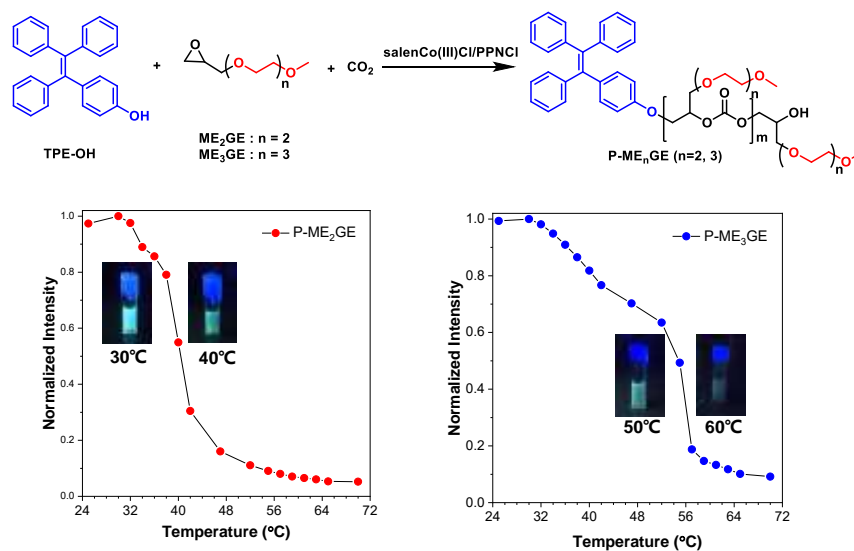
- [50] Han, S.; Hagiwara, M.; Ishizone, T. Synthesis of thermally sensitive water-soluble polymethacrylates by living anionic polymerizations of oligo(ethylene glycol) methyl ether methacrylates. *Macromolecules* **2003**, *36*, 8312-8319.
- [53] release from multi-responsive degradable poly(ether urethane) nanoparticles. *Biomater. Sci.* **2013**, *1*, 614-624
- [51] Ru, G.; Wang, N.; Huang, S.; Feng, J. ¹H HRMAS NMR Study on Phase Transition of Poly(N-isopropylacrylamide) Gels with and without Grafted Comb-Type Chains. *Macromolecules* **2009**, *42*, 2074-2078.
- [52] Wang, Y.; Wu, G.; Li, X.; Wang, Y.; Gao, H.; Ma, J. On-off switchable drug

Accepted Article

Entry for the Table of Contents

Construction of Self-Reporting Biodegradable CO₂-based Poly-carbonates for the Visualization of Thermoresponsive Behavior with Aggregation-Induced Emission Technology

Molin Wang, Enhao Wang, Han Cao, Shunjie Liu,* Xianhong Wang,* and Fosong Wang

Chin. J. Chem. **2021**, *39*, XXX–XXX. DOI: 10.1002/cjoc.202100XXX

Thermoresponsive polymers with simultaneous biodegradability and signal “self-reporting” outputs that meet for advanced applications are hard to obtain. In this work, we developed fluorescence signal “self-reporting” biodegradable thermoresponsive polycarbonates through the copolymerization of CO₂ and OEG-functionalized epoxides in the presence of hydroxyl-modified tetraphenylethylene (TPE-OH). The self-assemble of TPE-labeled polymer in aqueous solution resulted in fluorescence enhancement owing to the restriction of intramolecular motion mechanism of TPE. Further research indicated that temperature-controlled aggregation and dissociation of TPE moieties are the main reason for fluorescence intensity variations.